Antimicrobial Agents and Chemotherapy®

Rapid Evolution of Reduced Susceptibility against a Balanced Dual-Targeting Antibiotic through Stepping-Stone Mutations

Petra Szili,[a,f] Gábor Draskovits,[a] Tamás Révész,[a,e] Ferenc Bogár,[b,c] Dávid Balogh,[a] Tamás Martinek,[c] Lejla Daruka,[a] Réka Spohn,[a] Bálint Márk Vásárhelyi,[a] Márton Czikkely,[a,g] Bálint Kintses,[a,h] Gábor Grézal,[a] Györgyi Ferenc,[d] Csaba Pál,[a] Ákos Nyerges[a]

[a]Synthetic and Systems Biology Unit, Institute of Biochemistry, Biological Research Centre of the Hungarian Academy of Sciences, Szeged, Hungary
[b]MTA-SZTE Biomimetic Systems Research Group, University of Szeged, Szeged, Hungary
[c]Department of Medical Chemistry, University of Szeged, Szeged, Hungary
[d]Nucleic Acid Synthesis Laboratory, Biological Research Centre of the Hungarian Academy of Sciences, Szeged, Hungary
[e]Doctoral School of Theoretical Medicine, University of Szeged, Szeged, Hungary
[f]Doctoral School of Multidisciplinary Medical Sciences, University of Szeged, Szeged, Hungary
[g]Szeged Scientists Academy, Szeged, Hungary
[h]Department of Biochemistry and Molecular Biology, University of Szeged, Szeged, Hungary

ABSTRACT Multitargeting antibiotics, i.e., single compounds capable of inhibiting two or more bacterial targets, are generally considered to be a promising therapeutic strategy against resistance evolution. The rationale for this theory is that multitargeting antibiotics demand the simultaneous acquisition of multiple mutations at their respective target genes to achieve significant resistance. The theory presumes that individual mutations provide little or no benefit to the bacterial host. Here, we propose that such individual stepping-stone mutations can be prevalent in clinical bacterial isolates, as they provide significant resistance to other antimicrobial agents. To test this possibility, we focused on gepotidacin, an antibiotic candidate that selectively inhibits both bacterial DNA gyrase and topoisomerase IV. In a susceptible organism, *Klebsiella pneumoniae*, a combination of two specific mutations in these target proteins provide an >2,000-fold reduction in susceptibility, while individually, none of these mutations affect resistance significantly. Alarmingly, strains with decreased susceptibility against gepotidacin are found to be as virulent as the wild-type *Klebsiella pneumoniae* strain in a murine model. Moreover, numerous pathogenic isolates carry mutations which could promote the evolution of clinically significant reduction of susceptibility against gepotidacin in the future. As might be expected, prolonged exposure to ciprofloxacin, a clinically widely employed gyrase inhibitor, coselected for reduced susceptibility against gepotidacin. We conclude that extensive antibiotic usage could select for mutations that serve as stepping-stones toward resistance against antimicrobial compounds still under development. Our research indicates that even balanced multitargeting antibiotics are prone to resistance evolution.

KEYWORDS antibiotic resistance, genome engineering, gepotidacin

Antibiotic discovery has been driven by the need for new therapeutics that are not subject to rapid resistance development. Due to the rise of drug-resistant bacteria, the commercial success of antibiotic development is unpredictable (1, 2). Antibiotic combination therapy has long been suggested as a potential strategy to delay resistance evolution (3, 4). The rationale for this theory is that drugs with different modes of action generally require different mutations in the respective target genes to achieve resistance, and the simultaneous acquisition of multiple specific mutations is exceed-

FIG 1 Binding site analysis of gepotidacin based on directed evolution and molecular modeling. (A) Gepotidacin, a novel triazaacenaphthylene antibiotic candidate, inhibits DNA gyrase and topoisomerase IV in Gram-negative bacteria. (B and C) Ribbon representation of *E. coli*'s DNA gyrase and topoisomerase IV in complex with gepotidacin, based on molecular dynamics simulations. Inset shows the closeup view of gepotidacin (yellow) and its interacting residues (red) in a stick model. DNA is shown in magenta and blue. (D) The workflow of *in vivo* directed evolution of reduced susceptibility to gepotidacin in *K. pneumoniae* ATCC 10031.

ingly rare. Although successful in many cases, antimicrobial combination therapy suffers from several limitations (5, 6). Multitarget antibiotic strategy is an emerging alternative. There are multiple mechanisms by which antimicrobial compounds may inhibit multiple bacterial targets. In the case of hybrid drugs, two antibiotic pharmacophores with dissimilar targets are covalently linked to form one molecule. Other antibiotic compounds equipotently target two or more homologous proteins. Indeed, resistance to linezolid has typically been associated with multiple mutations in various numbers of copies of the genes encoding 23S rRNA, all of which have limited effects on resistance individually (7). Finally, they may target multiple nonoverlapping regions of a single bacterial protein. Currently, designing multitarget antibiotics is a major focus of the pharmaceutical industry, but until now, relatively few drugs have been demonstrated to achieve a balanced inhibition of multiple microbial targets (8–10). Due to the shortage of in-depth resistance studies, our knowledge on the tempo and mode of resistance development against multitarget antibiotics remains limited (11–13).

Gepotidacin (GSK2140944) is an exemplary candidate to study resistance evolution toward multitargeting antibiotics (Fig. 1A). Gepotidacin is a novel triazaacenaphthylene antibiotic candidate currently in phase 2b clinical trials (14, 15) and is expected to enter the clinical practice in the upcoming years (16, 17). The molecule inhibits bacterial DNA

gyrase and topoisomerase IV with a novel mode of action. Using a standard frequency-of-resistance test, recent studies have failed to identify resistant clones of *Neisseria gonorrhoeae* and *Escherichia coli* against this new compound (8, 18), suggesting that individual mutations cannot provide substantial resistance to gepotidacin. It is especially active against Gram-negative pathogens, such as *Klebsiella pneumoniae*. According to the WHO, infections caused by multidrug-resistant *Klebsiella* strains are emerging as a top-ranked challenge in the health care sector (19). In this work, we demonstrate that contrary to expectations, reduced susceptibility to gepotidacin evolves rapidly in *K. pneumoniae*, which has potential implications for the future clinical use of this new antibiotic candidate.

RESULTS

Molecular modeling with directed evolution accurately predicts the positions and impact of resistance mutations. Prior studies have demonstrated that gepotidacin selectively inhibits both bacterial DNA gyrase and topoisomerase IV by a unique mechanism (8, 16), but the exact molecular mechanisms of inhibition have not been thoroughly characterized. Therefore, we first sought to study the exact molecular interactions between gepotidacin and *Escherichia coli*'s DNA gyrase and topoisomerase IV protein complexes, using molecular modeling (see Materials and Methods; see also Note S1 in the supplemental material). Molecular dynamics simulations capture the atomic interactions between the drug and the target protein in time (Fig. S1). The analysis has revealed that D82 in the GyrA subunit of DNA gyrase and the homologous position, D79 of the ParC subunit of topoisomerase IV, form an intermolecular salt bridge with gepotidacin (Fig. 1B and C, S1, and S2 and Note S2). Therefore, mutations at these binding sites are expected to provide reduced susceptibility to gepotidacin, and it was indeed so (see below).

Previously, we subjected the potential target genes to a single round of directed evolution with random genomic mutation (DIvERGE) mutagenesis in *E. coli* and then subjected the mutant library to gepotidacin stress, followed by sequencing of the isolates with reduced susceptibility (18). As gepotidacin has not entered clinical use and, thus, its clinical breakpoint is not established, we defined reduced susceptibility to gepotidacin as the MIC value that is equal or higher than the peak plasma concentration of the drug (9 μg/ml [14]). In our current work, the analysis has been repeated in *K. pneumoniae* using nearly identical experimental settings (Fig. 1D). The results of the mutagenesis assays are qualitatively the same for the two species, as D82 within the GyrA subunit and D79 of the ParC subunit are found to be mutated in all the clones isolated, and no further mutations have been found (Table S4). Moreover, subsequent saturation mutagenesis of the two mutational hot spots has recapitulated that the combination of these two specific mutations (GyrA D82N and ParC D79N) is responsible for a high-level reduction of susceptibility to gepotidacin (Table S4).

To understand the molecular mechanisms behind the reduced susceptibility, we have computationally modeled the molecular interactions between gepotidacin and asparagine mutants at the GyrA D82 and ParC D79 positions using molecular dynamics simulations and the molecular mechanics/generalized born surface area (MM-GBSA) (20) method. MM-GBSA has predicted that the observed mutations (GyrA D82N and ParC D79N) weaken the interaction between the target proteins and gepotidacin (Fig. S1). Thus, the combination of DIvERGE mutagenesis assays and molecular dynamics simulations has revealed the putative binding sites for gepotidacin in DNA gyrase and topoisomerase IV protein complexes. Furthermore, the disruption of an indispensable salt bridge between the drug and its two binding sites resulted in high-level reduction of susceptibility in *K. pneumoniae*.

Exceptionally strong synergism between mutations is associated with reduced susceptibility. Next, we have studied the individual and combined effects of these mutations on susceptibility. For this purpose, the mutations were inserted individually into the genomes of *E. coli* K-12 MG1655 and *K. pneumoniae* ATCC 10031. The double mutants were found to display >560- and 2,080-fold reductions in gepotidacin sus-

TABLE 1 Gepotidacin and ciprofloxacin MICs of single-step mutations and their combination in *Escherichia coli* K-12 MG1655 and *Klebsiella pneumoniae* ATCC 10031[a]

|	MIC (µg/ml) for:	
Strain	Gepotidacin	Ciprofloxacin
E. coli K-12 MG1655		
Wild type	0.25	0.016
GyrA D82N mutant	0.5	0.125
ParC D79N mutant	0.5	0.016
GyrA D82N ParC D79N mutant	>256	0.25
K. pneumoniae subsp. *pneumoniae* ATCC 10031		
Wild type	0.063	0.004
GyrA D82N mutant	0.5	0.063
ParC D79N mutant	0.125	0.008
GyrA D82N ParC D79N mutant	256	0.063

[a]Growth inhibition was determined by OD_{600} measurements of the bacterial culture after 18 h of incubation in the presence of the corresponding drug concentration, according to the EUCAST guidelines (73, 74). The results presented here are the means of 9 independent replicates.

ceptibility levels compared to the corresponding wild-type strains of *E. coli* and *K. pneumoniae*, respectively (Table 1) (18). In contrast, the single mutants were found to show no considerable changes in gepotidacin susceptibility in both species (Table 1). These findings are consistent with prior single-step resistance selection studies that failed to recover mutants with significant resistance (8, 18).

Fitness cost of decreased gepotidacin susceptibility is limited. Antibiotic resistance typically induces a fitness cost in the form of reduced bacterial growth rates (21), and such costs shape the long-term stability of antibiotic-resistant populations (22–24). Thus, we have investigated the fitness effects of target-mediated reduction of susceptibility to gepotidacin in *K. pneumoniae*. To this aim, we have studied the wild-type and mutant *K. pneumoniae* strains, with the latter carrying mutations associated with reduced susceptibility to gepotidacin or fluoroquinolones.

The fluoroquinolone resistance-causing mutations in point are widespread in clinical isolates (25–27) and affect the same genes (namely, *gyrA* and *parC*); therefore, they provide a benchmark to estimate the fitness costs compared to the wild-type strain. Relative fitness was estimated by pairwise competition experiments between the wild-type strain and a specific mutant strain in nutrient-rich antibiotic-free bacterial medium (Mueller-Hinton II broth [MHBII]) at 37°C. Using established protocols, we have found that the mutation combination of GyrA D82N and ParC D79N, which confers reduced susceptibility to gepotidacin, significantly decreases fitness in *K. pneumoniae*. However, the fitness cost of gepotidacin resistance-associated mutations is comparable to the fitness cost of canonical clinically relevant fluoroquinolone resistance-causing mutations. Importantly, the ParC D79N mutation is found to confer no measurable fitness cost individually (Fig. 2A). Our findings remained the same when active human blood serum was added to the medium (data not shown).

Mutants with reduced susceptibility to gepotidacin display no changes in virulence in a murine infection model. We next investigated whether mutants with reduced susceptibility to gepotidacin display reduced virulence *in vivo*. As drug-resistant *K. pneumoniae* is frequently responsible for wound and systemic infections, we have studied a murine thigh wound infection model (28, 29). Specifically, we have examined the wound colonization capacity of the wild-type strain, as well as that of representative *K. pneumoniae* mutants with reduced gepotidacin or ciprofloxacin susceptibility. For this purpose, the wild-type strain and each isogenic mutant strain were inoculated into the thigh tissue of female ICR mice ($n = 5$). After 26 h, bacterial colonization was determined by plating thigh tissue homogenates to MHBII agar plates. No significant decrease in *in vivo* virulence was observed for any of the mutants compared to the wild-type strain (Fig. 2B). It is worth noting, however, that performing *in vivo* competition experiments in a mouse infection model would also be desirable to
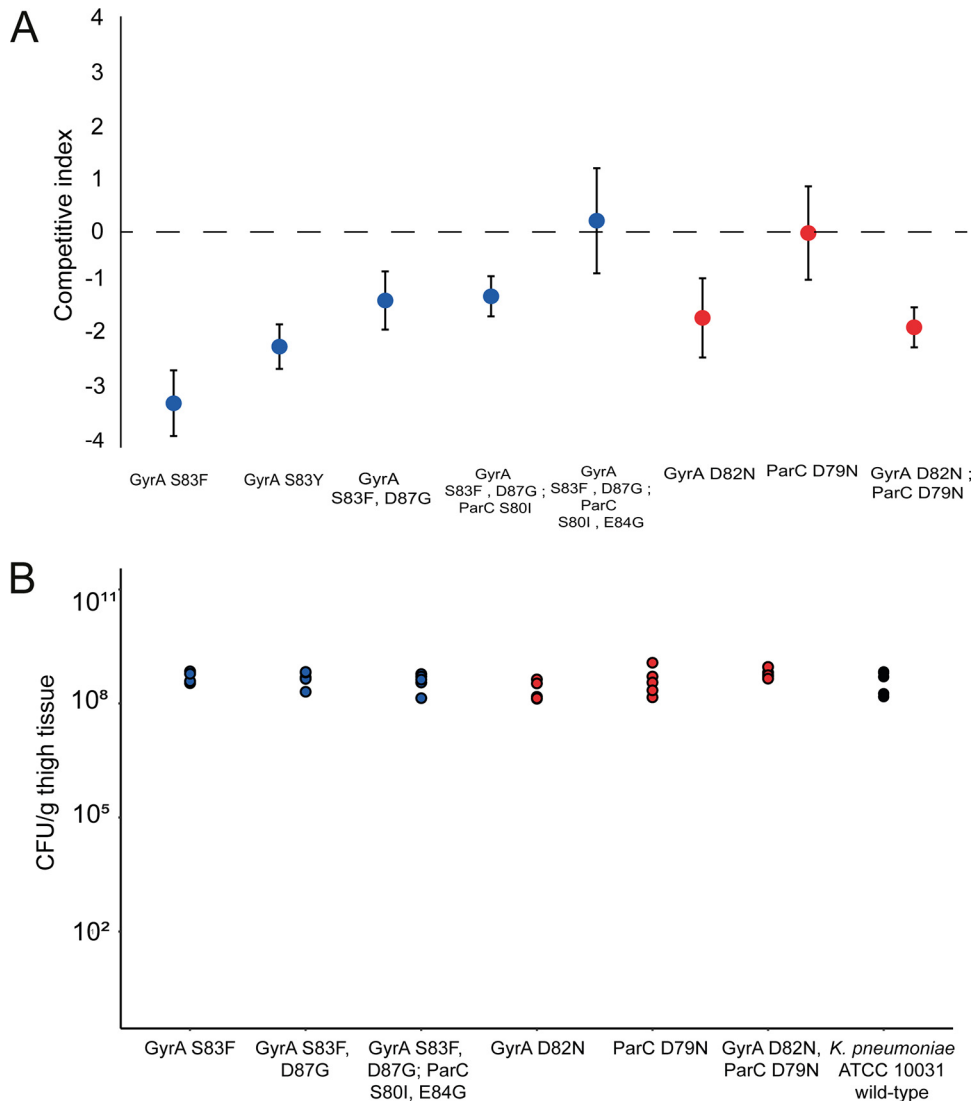
FIG 2 Fitness cost and virulence of bacteria with reduced susceptibility to gepotidacin. (A) *In vitro* competition between mutant and wild-type *Klebsiella pneumoniae*. Isogenic mutants of *Klebsiella pneumoniae* ATCC 10031 carrying either a mutation combination conferring reduced susceptibility to gepotidacin or its single-step constituents (red), or clinically occurring fluoroquinolone resistance-associated mutations (blue) competed against the wild-type strain. In competition assays, a competitive index of <0 indicates that the wild-type population outcompetes the mutant population, and conversely, a competition index of >0 indicates that the mutant population outcompetes the wild-type population. Error bars indicate the standard deviation (SD) based on five biological replicates. (B) Virulence of *Klebsiella pneumoniae* mutants and the wild-type strain in a murine thigh infection model. Shown are the bacterial burdens in infected thigh tissues after 26 h of infection caused by wild-type *Klebsiella pneumoniae* ATCC 10031 (black) or isogenic mutants carrying either mutations causing reduced susceptibility to gepotidacin or its single-step constituents (red), or clinically occurring mutations associated with fluoroquinolone resistance (blue). The bacterial burden was assayed in CFU per gram of tissue ($n = 5$ animals per data point, see Materials and Methods for details). No mutants were found to display a significant difference in virulence compared to the wild-type strain (*t* test, $P > 0.05$ for all pairwise comparisons).

further characterize the *in vivo* virulence of the mutations causing reduced susceptibility to gepotidacin, and in future work, we plan to analyze that.

Cross-resistance analysis between gepotidacin and ciprofloxacin. Several prior works demonstrate that certain resistance mutations are present in bacterial populations long before being exposed to an antibiotic in point. Thus, we hypothesized that prolonged use of other antibiotics might select for mutations that serve as stepping-stones toward reduced susceptibility to gepotidacin. The best candidate antibiotic family is fluoroquinolones, as they are widely employed in clinical practice, and similarly

to gepotidacin, they target the gyrase-topoisomerase protein complexes, albeit with a notably different molecular mechanism (17, 30). Moreover, the putative binding sites of gepotidacin and fluoroquinolones on the GyrA protein are adjacent to each other, separated by a single amino acid only (Fig. 1B) (31–33). Despite the functional similarities between these drug classes, a prior paper reported that fluoroquinolone-resistant clinical isolates displayed no cross-resistance to gepotidacin (17). To reinvestigate this issue, we have focused on ciprofloxacin, a widely employed and well-characterized fluoroquinolone drug. Several ciprofloxacin resistance-conferring mutations and mutation combinations in clinical isolates provide no relevant cross-resistance against gepotidacin (Table S5). More surprising results have emerged by testing the effect of mutations conferring reduced susceptibility to gepotidacin on ciprofloxacin susceptibility. We have found that the GyrA D82N single-mutant strain displays an over 16-fold increase in ciprofloxacin resistance level compared to that of the wild-type *K. pneumoniae* ATCC 10031 strain. This finding is even more remarkable if we consider that the same mutation confers only a 2-fold increase in gepotidacin MIC level. As might be expected, the GyrA D82N and ParC D79N double mutants also display significant resistance to ciprofloxacin (Table 1).

Our findings raise the possibility that the D82N mutation of GyrA might be present in fluoroquinolone-resistant clinical isolates, rendering the subsequent emergence of double mutants with reduced susceptibility to gepotidacin feasible. We have systematically investigated the prevalence of the GyrA D82N and ParC D79N mutations in currently available sequence databases (as of 9 October 2018). A systematic sequence search has revealed that both mutations occur in a wide range of Gram-negative and Gram-positive bacteria (Table S2, Fig. S4, and File S1), including fluoroquinolone-resistant clinical isolates of *E. coli* (34) and other species belonging to the *Salmonella*, *Mycoplasma*, *Clostridium*, *Citrobacter*, *Streptococcus*, and *Neisseria* genera. *Neisseria* and *Streptococcus* are especially noteworthy, as infections caused by organisms of these genera are reported to be the targets of gepotidacin in recent clinical trials (14, 15, 35). These results indicate that several clinically occurring human pathogens require only a single extra mutation to evolve highly reduced susceptibility to gepotidacin.

Ciprofloxacin stress selects for reduced susceptibility to gepotidacin in the laboratory. To establish further that ciprofloxacin promotes reduced susceptibility to gepotidacin, we have initiated laboratory evolution under ciprofloxacin stress with wild-type *K. pneumoniae* ATCC 10031, as well as the wild-type and Δ*mutS* mutant strains of *E. coli* K-12 MG1655. The previously established protocol aims to maximize the level of drug resistance in the evolving populations that develop in a fixed time period (36–38), being approximately 116 generations in our case. Six parallel evolving populations of each strain were exposed to gradually increasing concentrations of ciprofloxacin. In line with previous clinical and laboratory studies (30, 39), ciprofloxacin resistance was seen to emerge quickly in our experiments (Fig. 3A), especially in Δ*mutS* hypermutator lineages. Despite the short time frame, all *E. coli* and *K. pneumoniae* populations reached ciprofloxacin resistance levels equal to or above the EUCAST clinical breakpoint (40) (Fig. 3A and B). Three randomly selected ciprofloxacin-resistant lineages per strain were selected for gepotidacin MIC measurements. Strikingly, all have been found to display a >64- to 1,058-fold decrease in gepotidacin susceptibility level compared to the corresponding control strains (Fig. 3B). Next, we carried out whole-genome sequence analysis of 2 and 3 evolved lineages derived from *E. coli* K-12 MG1655 and *K. pneumoniae* ATCC 10031, respectively. Although these lineages display markedly reduced gepotidacin susceptibilities (Fig. 3B), they do not carry mutations at GyrA D82 or ParC D79, suggesting that multiple other mutations may also select for reduced susceptibility to gepotidacin. Indeed, whole-genome sequencing has revealed that these ciprofloxacin-resistant lineages carry putative resistance mutations in genes involved in membrane efflux (*acrR, soxR,* and *marR*) and the general stress response (*cusS* and *rpoB*) (Table S3). Overall, these results strongly suggest that long-term exposure to ciprofloxacin stress promotes reduced susceptibility to gepotidacin.
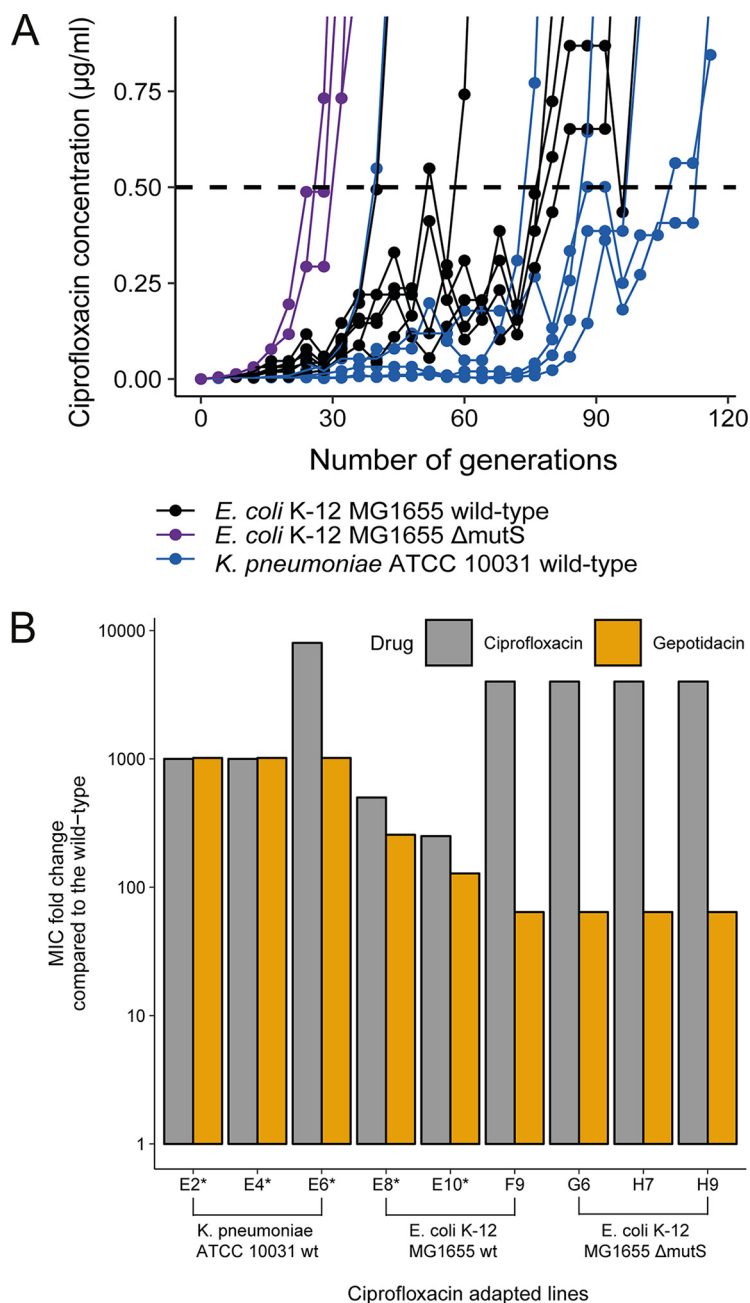
FIG 3 Adaptive laboratory evolution of *Klebsiella pneumoniae* and *Escherichia coli* under ciprofloxacin stress. (A) Antibiotic concentrations at which *K. pneumoniae* ATCC 10031 as well as *E. coli* K-12 MG1655 wild-type and Δ*mutS* hypermutator strains were able to grow under increasing ciprofloxacin stress as a function of time (number of cell generations). Dashed line represents the clinical breakpoint of ciprofloxacin resistance according to EUCAST (40). (B) Relative resistance level of the evolved lines against ciprofloxacin (gray bars) and gepotidacin (yellow bars) compared to the wild type at the end of the adaptive laboratory evolution. Asterisk (*) indicates that the evolved line was subjected to whole-genome sequence analysis to uncover mutational processes behind the reduced susceptibility.

DISCUSSION

In this work, we have primarily focused on studying the evolution of reduced susceptibility to gepotidacin in *Klebsiella pneumoniae*. As gepotidacin shows excellent potency against Gram-negative bacteria (16, 17, 41), it could be a last-resort drug to treat multidrug-resistant *Klebsiella* infections. However, we have demonstrated that two specific mutations in the genes encoding gepotidacin's targets can provide drastically

reduced susceptibility in multiple enterobacterial species (18) (see also Table 1). These two mutations (GyrA D82N and ParC D79N) overlap the predicted binding sites of the drug and show extreme synergism. By abolishing indispensable drug-target interactions, they confer an >2,000-fold reduction in susceptibility, but individually, they have only limited effects on susceptibility to gepotidacin. Alarmingly, the *K. pneumoniae* double mutant strain is as virulent as the wild type in a mouse infection model, suggesting that these mutations might have clinical significance. Indeed, *Neisseria gonorrhoeae* strains with reduced susceptibility to gepotidacin that were isolated in a human clinical phase 2b trial carried a ParC D86N mutation (35) that corresponds to the homologous ParC D79N mutation in *E. coli*.

According to what we term the "stepping-stone" hypothesis, the prolonged clinical deployment of certain antibiotics may select for variants with an elevated potential to evolve resistance to new antimicrobial agents. For example, in *Staphylococcus aureus*, the genetic alteration responsible for methicillin resistance had emerged due to the selective pressure of first-generation beta-lactams, such as penicillin, years before methicillin was first applied in clinical practice (42). Hierarchical resistance acquisition is also predominant during the evolution of resistance to fluoroquinolone antibiotics (43, 44). Furthermore, the by-products of drug degradation were also shown to promote resistance development against clinically applied antibacterials (45).

To investigate the feasibility of the stepping-stone hypothesis, here, we have focused on ciprofloxacin, a widely employed and well-characterized fluoroquinolone antibiotic (46). Similarly to gepotidacin, mutations in GyrA and ParC contribute to resistance to ciprofloxacin. Strikingly, mutations linked to reduced susceptibility to gepotidacin (i.e., GyrA D82N and ParC D79N) increase resistance to ciprofloxacin and have been detected in clinical isolates of ciprofloxacin-resistant bacteria, including strains of *N. gonorrhoeae*, *Streptococcus*, and *Salmonella enterica*. Therefore, these isolates are expected to require only one extra mutational step to develop reduced susceptibility to gepotidacin.

The stepping-stone hypothesis may have general implications. For example, zoliflodacin (ETX0914), a novel bacterial topoisomerase inhibitor, has just completed a human phase 2 clinical trial (47). It shows promising activity against multidrug-resistant infections, including those caused by *N. gonorrhoeae* (48). However, in this species, mutations in GyrB have been reported to confer zoliflodacin resistance (49), and one of these zoliflodacin-resistant mutants (D429N) has already been detected in clinical populations (50). As the homologous GyrB mutation (D426N) in *E. coli* confers resistance to fluoroquinolones (18), fluoroquinolone agents might have incidentally selected for reduced susceptibility to zoliflodacin as well. Consistent with this hypothesis, naturally occurring zoliflodacin-resistant variants were also found to be highly resistant to fluoroquinolones (50).

In summary, our work demonstrates that despite a balanced *in vivo* targeting of multiple proteins, high-level resistance can rapidly emerge to antibiotics when the drug molecule's inhibitory effect depends merely on interactions with a few indispensable amino acids. It is an open issue whether this conclusion holds for a drug that inhibits two completely novel targets. Moreover, based on adaptive laboratory evolution and clinical data, we propose that target gene mutations conferring resistance to fluoroquinolones can facilitate resistance evolution to novel topoisomerase-targeting antimicrobials, including gepotidacin. Therefore, existing resistant bacteria could serve as an immediate source of novel resistance mechanisms. As a more general concept, our work indicates that even drugs executing a balanced multitargeting of bacterial proteins are prone to resistance, and multitargeting itself does not preclude the appearance of high-level resistance to antimicrobials. Considering that a quarter of the antibiotics currently under clinical development target bacterial topoisomerases (https://www.pewtrusts.org/en/research-and-analysis/data-visualizations/2014/antibiotics-currently-in-clinical-development), further research is warranted to test this scenario.

MATERIALS AND METHODS

Media and antibiotics. For general growth of bacteria and electrocompetent cell preparation, lysogeny broth (LB) medium was used (10 g tryptone, 5 g yeast extract, 5 g sodium chloride per liter of water). For cell recovery after electroporation, we applied Terrific broth (TB; 24 g yeast extract, 12 g tryptone, 9.4 g K_2HPO_4, and 2 g KH_2PO_4 per liter of water). For antimicrobial susceptibility tests and selection of resistant variants, cation-adjusted Mueller-Hinton II broth (MHBII) was used. To prepare MHBII broth, 22 g of MHBII powder (Becton, Dickinson and Co.) was dissolved in 1 liter of water (3 g beef extract, 17.5 g acid hydrolysate of casein, and 1.5 g starch). MHBII agar was prepared by the addition of 14 g Bacto agar to 1 liter bacterial MHBII broth. Bacterial media were sterilized by autoclaving 15 min at 121°C. To distinguish *lacZ* knockout strains and wild-type strains, sterile solutions of X-Gal (5-bromo-4-chloro-3-indolyl-β-D-galactopyranoside) and IPTG (isopropyl-β-D-1-thiogalactopyranoside) were added to the MHBII agar medium after autoclaving. The final X-Gal and IPTG concentrations in the medium were 40 mg/liter and 0.2 μM, respectively. Antibiotics and chemicals were ordered from Sigma-Aldrich (ampicillin, kanamycin, chloramphenicol, X-Gal, and IPTG), Fluka Analytical (ciprofloxacin), and MedChem-Express (gepotidacin).

Oligonucleotides. The sequences of all synthetic DNA oligonucleotides are listed in File S1. Oligonucleotides were synthesized at the Nucleic Acid Synthesis Laboratory of the Biological Research Centre of the Hungarian Academy of Sciences. Soft-randomized DIvERGE oligonucleotides were manufactured according to a previously described soft-randomization protocol (18). PCR primers were purified with standard desalting, while mutagenic oligonucleotides were purified with high-performance liquid chromatography (HPLC). Lyophilized oligonucleotides were dissolved in 1× Tris-EDTA (TE) buffer (pH 8) (Integrated DNA Technologies) at a final concentration of 100 μM. DIvERGE oligonucleotides were dissolved in 0.5× TE buffer at a final concentration of 500 μM. The dissolved oligonucleotides were stored at −20°C.

Homology model building. The crystal structure of *Staphylococcus aureus* in complex with compound GSK945237 (PDB code: 5NPP [75]; resolution, 2.22 Å) was chosen as the template to build a homology model of *Escherichia coli* DNA gyrase using Prime from the Schrödinger package (76, 77). GSK945237 is also a member of novel bacterial topoisomerase inhibitors (NBTI); therefore, its binding position can serve as a template in our study. The homology model of topoisomerase IV of *Escherichia coli* was created by using the X-ray structure of *Klebsiella pneumoniae* in complex with levofloxacin (PDB code 5EIX [78]; resolution, 3.35 Å) as the template. In the case of DNA gyrase, the DNA chain and the ligand GSK945237 (with both binding poses) were directly transferred from the template PDB structure 5NPP. Since the DNA binding of the two enzyme shows high similarity, the DNA chain and the ligand were also transferred from 5NPP to the homology model of topoisomerase IV after fitting the backbone atoms of the two proteins. In both cases, the protein DNA contacts were checked and corrected separately using local conformation search and minimization.

Computational docking of gepotidacin. We docked gepotidacin (ChemSpider ID 34982930) into the DNA gyrase and topoisomerase IV homology models using Glide from the Schrödinger package (51). The protonation state of gepotidacin was selected as the main species obtained from the pK_a calculation using the calculator plugin of the Marvin 16.2.1 program (Chemaxon). For glide docking, we used an OPLS3 force field (52) and the standard precision procedure with flexible ligand geometries and enhanced conformational sampling. Based on the high similarity of the modes of action of GSK945237 and gepotidacin (41), we picked the docking pose of gepotidacin that was most similar to the binding pose of GSK945237 in the 5NPP structure. This procedure was repeated for the other docking pose of GSK945237 as well. Finally, the binding site (defined as residues closer than 5 Å to the ligand) geometry together with the docked ligand were optimized. We followed the same steps with the two homology models.

Molecular dynamics simulations of gepotidacin bound DNA gyrase and DNA topoisomerase IV complexes. To perform molecular dynamics-based binding mode analysis for gepotidacin at both of its targets, we first parametrized the complex formed by gepotidacin-DNA and its corresponding target (DNA gyrase and topoisomerase IV, respectively). For parametrization, we used an OPLS3 force field (52). Next, this system was solvated using the simple point charge (SPC) explicit water model (53) within an orthorhombic box 10 Å apart. On the course of simulations, NaCl at a 0.15 M final concentration was used to mimic the physiological conditions. One hundred-nanosecond molecular dynamics calculations were carried out on these systems at constant volume and temperature (NVT) using the Desmond molecular dynamics code (54). Snapshots of these simulations were used as a conformational ensemble in mutation-induced binding free energy change calculations.

Estimation of mutation-induced binding free energy changes. Asparagine mutation-induced changes in the binding affinity ($\Delta\Delta G_B$) of gepotidacin at the GyrA D82 and ParC D79 positions were calculated as the difference in their binding free energies in the mutated (MUT) and wild-type (WT) enzymes ($\Delta\Delta G_B = \Delta G_B^{MUT} - \Delta G_B^{WT}$). This affinity change was estimated by using the residue scanning module of the Bioluminate package (55) and was based on a molecular mechanics-generalized Born surface area (MM-GBSA) approximation (18). Specifically, we estimated the binding free energy of a ligand (ΔG) by using the single trajectory approach (20) in which a single molecular dynamics simulation of the protein-ligand complex is completed first and sample geometries are collected from the trajectory to represent the possible binding conformations. The ΔG value is calculated for every single geometry as

$$\Delta G = G_{PL} - G_P - G_L$$

where G_{PL}, G_P, and G_L are the energy of the protein ligand complex, protein, and ligand, respectively. These energy values are calculated as

$$G = G_{MM} + G_{Solv}$$

where G_{MM} is the calculated molecular mechanics energy for the force field applied and G_{Solv} is the solvation energy in the generalized Born approximation. Different variations of this method are widely used in large-scale drug design studies (56–58), as it accurately predicts mutational effects in drug-protein interaction analyses with a manageable computational demand (see, e.g., references 59 and 60). In our study, MM-GBSA calculations were carried out with the thermal_mmgbsa.py script in the Schrödinger package (55) from 100 evenly spaced structures from the second 50 ns of our previously performed molecular dynamics simulation between the wild-type enzyme (DNA gyrase and topoisomerase IV) and gepotidacin.

Plasmid construction. To perform single-stranded DNA (ssDNA) recombineering and DIvERGE in *K. pneumoniae* ATCC 10031, we generated a novel version of pORTMAGE, termed pORTMAGE311B. This plasmid possesses a tightly regulated XylS-Pm regulator/promoter-based λ Beta and *E. coli* MutL E32K coexpression system. On pORTMAGE, the expression of MutL E32K of *E. coli* abolishes methyl-directed mismatch repair (MMR) during the time period of oligonucleotide incorporation into the bacterial genome (61). pORTMAGE311B ensured functionality at 37°C and the rapid inducibility of λ Beta and *E. coli* MutL E32K by the addition of 1 mM *m*-toluic acid as an inducer. The temporal coexpression of λ Beta and MutL E32K also limits off-target mutagenic effects on the course of genome editing. The construction of pORTMAGE311B was performed by introducing the coding sequence of the dominant *E. coli* *mutL*(E32K) allele to the pSEVA258*beta* plasmid (62). To this aim, *mutL*(E32K) was PCR amplified from pORTMAGE2 (61) using the primers RBE32KF and XE32KR. The PCR product was then purified and digested with BamHI and XbaI. Next, the resulted fragment was cloned downstream of *beta* within pSEVA258*beta*. Finally, the successful assembly of the plasmid was verified by PCR and confirmed by capillary sequencing. pORTMAGE311B was also deposited to Addgene (no. 120418).

DIvERGE in *Klebsiella pneumoniae*. DIvERGE in *Klebsiella pneumoniae* ATCC 10031 was carried out according to a previously described DIvERGE workflow (18), with minor modifications. Briefly, *K. pneumoniae* cells carrying pORTMAGE311B plasmid were inoculated into 2 ml LB medium plus 50 μg/ml kanamycin and were grown at 37°C and 250 rpm overnight. From this starter culture, 500 μl stationary-phase culture was inoculated into 50 ml LB medium plus 50 μg/ml kanamycin and grown at 37°C under continuous shaking at 250 rpm. Induction was initiated at an optical density at 600 nm (OD_{600}) of 0.4 by adding 50 μl of 1 M *m*-toluic acid (dissolved in 96% ethyl alcohol; Sigma-Aldrich). Induction was performed for 30 min at 37°C. After induction, cells were cooled on ice for 15 min. Next, cells were washed 3 times with 50 ml sterile ice-cold ultrapure distilled water. Finally, the cell pellet was resuspended in 800 μl sterile ultrapure distilled water and kept on ice until electroporation.

To perform DIvERGE, and separately, the saturation mutagenesis of GyrA D82 and ParC D79, the corresponding *gyrA*- and *parC*-targeting oligonucleotides were equimolarly mixed at a final concentration of 500 μM, and 2 μl of this oligonucleotide mixture was added to 40 μl electrocompetent cells in 10 parallel samples. Following the electroporation of each sample, the 10 parallel samples were pooled, and immediately after electroporation, cells were suspended in 50 ml TB to allow for cell recovery. After a 1-h recovery period at 37°C and 250 rpm, an additional 50 ml LB medium along with 50 μg/ml (final concentration) kanamycin was added. Next, cells were grown at 37°C and 250 rpm for 24 h. To select clones with reduced susceptibility to gepotidacin from this DIvERGE library, 500 μl cell library was spread to 6 μg/ml gepotidacin-containing MHBII agar plates, and the plates were incubated at 37°C for 48 h. Finally, 10 randomly selected colonies were analyzed by capillary sequencing (oligonucleotides KPGA1F and KPGA1R, and KPPC1F and KPPC1R) from both antibiotic-selected cell libraries.

Engineering mutations associated with reduced susceptibility to gepotidacin in *Escherichia coli*. To assess the phenotype of mutations associated with reduced susceptibility to gepotidacin, we individually reconstructed both GyrA D82N and ParC D79N mutations in *E. coli* K-12 MG1655. We utilized a previously described CRISPR-assisted multiplex automated genome engineering (MAGE) protocol to integrate mutations and counterselect against the wild-type genotype (63, 64). Briefly, cells containing pORTMAGE2 (Addgene no. 72677) were transformed with pCas9 (Addgene no. 42876) and were grown in LB plus 100 μg/ml ampicillin and 20 μg/ml chloramphenicol broth at 30°C. Next, pCRISPR plasmids (Addgene no. 42875) were constructed with CRISPR RNA (crRNA) sequences targeting the wild-type *gyrA* and *parC* loci in the vicinity of D82 and D79, according to a previously described protocol (oligonucleotides ECGACRF1 and ECGACRR1, and ECPCCRF1 and ECPCCRR1, respectively). Following plasmid construction, the correct clones were identified by capillary sequencing. To integrate the GyrA D82N and ParC D79N mutations into the chromosome of *E. coli*, induced pORTMAGE2 and pCas9-carrying cells were prepared and made electrocompetent. Next, simultaneously, 100 ng of the corresponding pCRISPR plasmid and 200 pmol oligonucleotide (MGYRA82N or MPARC79N) per 40 μl electrocompetent cells were electroporated. Cells were allowed to recover in 1 ml TB medium and grown in 5 ml LB plus 100 μg/ml ampicillin plus 20 μg/ml chloramphenicol broth at 30°C overnight and then spread to LB plus 50 μg/ml kanamycin plus 20 μg/ml chloramphenicol agar plates. Finally, the presence of the correct mutations was identified by capillary sequencing of the oligonucleotide targets (oligonucleotides 25922Ga1 and 25922Ga3, and 25922Pc1 and 25922Pc3).

Engineering isogenic *Klebsiella* and *Salmonella* strains carrying mutations associated with reduced susceptibility to gepotidacin and fluoroquinolones. To investigate mutational effects on antibiotic susceptibility and growth phenotypes, mutations and mutation combinations linked to reduced susceptibility to gepotidacin and ciprofloxacin were reconstructed in *K. pneumoniae* ATCC 10031 and in *Salmonella enterica* subsp. *enterica* serovar Typhimurium. To this aim, specific point mutations (see File S1) were inserted into the chromosome of *K. pneumoniae* by pORTMAGE recombineering (18, 61). Briefly, pORTMAGE recombineering was performed using pORTMAGE311B (Addgene no. 120418). One microliter of 100 μM the corresponding oligonucleotides or oligonucleotide mixtures was used for ssDNA

recombineering in appropriate combinations to create mutations linked to reduced susceptibility to gepotidacin and ciprofloxacin. Following recombineering, cells were allowed to grow overnight in TB medium at 37°C and 250 rpm. Next, variants carrying ciprofloxacin resistance-conferring mutations were selected on plates with LB plus 100 ng/ml ciprofloxacin, while mutants carrying the GyrA D82N and ParC D79N mutation combination were selected on plates with MHBII plus 6 μg/ml gepotidacin agar. Cells carrying individual mutations associated with reduced susceptibility to gepotidacin were plated onto LB plus 50 μg/ml kanamycin agar. To obtain individual colonies, cultures from each recombineering population were diluted, and appropriate dilutions were spread to agar plates. Plates were incubated at 37°C, and individual colonies were genotyped by allele-specific PCR (using oligonucleotides KPA82ASF and KPA82ASR, and KPC79ASF and KPC79ASR). Finally, positive clones were confirmed by capillary sequencing of the oligonucleotide target region. The reconstruction of the clinically prevalent GyrA D82 mutation in combination with a ParC D79N mutation in *Salmonella enterica* subsp. *enterica* serovar Typhimurium LT2 was conducted similarly to the reconstruction of specific mutations in *K. pneumoniae*. Briefly, pORTMAGE311B-containing induced *S. enterica* cells were made electrocompetent and transformed with 1 μl of SE_GA_D82N and SE_PC_D79N oligonucleotides that integrated the corresponding GyrA D82N and ParC D79N mutations into the bacterial chromosome. Next, mutants were selected on MHBII plus 6 μg/ml gepotidacin agar plates at 37°C. Finally, the presence of the two mutations was identified and validated by capillary sequencing using the SEGAF1 and SEGAR1, and SEPCF1 and SEPCR1 oligonucleotides.

Adaptive laboratory evolution of ciprofloxacin resistance. Adaptive laboratory evolution experiments followed an established protocol for automated laboratory evolution (65) and aimed to maximize the drug resistance increment during a fixed time period. At each transfer step, 10^7 bacterial cells were transferred to a new culture, and adaptation was performed by passaging 6 independent populations of *Klebsiella pneumoniae* ATCC 10031 wild-type, *Escherichia coli* K-12 MG1655 wild-type, and *Escherichia coli* K-12 MG1655 $\Delta mutS$ strains in the presence of increasing ciprofloxacin concentrations. Experiments were conducted in 96-well plates in MHBII medium, utilizing a checkerboard layout to minimize and monitor cross-contamination. These 96-well deep-well plates (0.5 ml, polypropylene, V-bottom) were covered with sandwich covers (Enzyscreen BV) to ensure an optimal oxygen exchange rate and limit evaporation and were shaken at 150 rpm at 37°C. Twenty microliters of each evolving culture was transferred in parallel into four independent wells containing 350 μl fresh medium and increasing concentrations of gepotidacin and ciprofloxacin (i.e., 0.5×, 1×, 1.5×, and 2.5× the concentrations of the previous concentration step). Following cell transfer, each culture was allowed to grow for 48 h. At each transfer, cell growth was monitored by measuring the optical density at 600 nm (OD_{600}) (Biotek Synergy 2). Only populations with (i) vigorous growth (i.e., OD_{600}, >0.25) and (ii) the highest drug concentration were selected for further evolution. Accordingly, only one of the four populations was retained for each independently evolving strain. This protocol was designed to avoid population extinction and to ensure that populations with the highest level of resistance were propagated further during evolution. Samples from each transfer were frozen in 15% dimethyl sulfoxide (DMSO) at -80°C for further analysis. Adaptation of an individual population was terminated when the antibiotic concentration in the given well would have exceeded 200 μg/ml after the transfer. Cells from these highly drug-resistant populations were frozen after the addition of 15% dimethyl sulfoxide (DMSO) and were kept at -80°C. Following adaptation, cells from each final population were spread onto MHBII agar plates, and individual colonies were isolated.

Whole-genome sequencing of adapted lines. Following adaptive laboratory evolution of ciprofloxacin resistance in *K. pneumoniae* ATCC 10031 and *E. coli* K-12 MG1655, single colonies from three adapted lines were subjected to whole-genome sequencing on an Illumina HiSeq 4000 platform. Prior to sequencing, genomic DNA (gDNA) was isolated from each adapted line and the corresponding wild-type strain by using the GenElute gDNA isolation kit (Sigma-Aldrich), according to the manufacturer's instructions. To perform DNA sequencing, sequencing libraries were constructed from the gDNAs by fragmenting samples to a mean fragment length of 300 bp. Next, sequencing libraries were prepared by using a TruSeq DNA PCR-free library prep kit (Illumina). Finally, sequencing libraries were sequenced on a single sequencing lane of an Illumina HiSeq 4000 system using a HiSeq 3000/4000 SBS kit (300 cycles, FC-410-1003; Illumina) to generate 2 × 150-bp paired-end reads. Following sequencing, in order to determine the variants and to annotate the mutations, we mapped sequencing reads to their corresponding reference genomes with the mem subcommand of bwa 0.7.12-r1039 (Burrows-Wheeler Aligner [66]). The single-nucleotide polymorphisms (SNPs) and indels were called with VarScan v2.3.9 (67) with the following parameters: min-reads2 = 4, min-coverage = 30, min-var-freq = 0.1, min-freq-for-hom = 0.6, min-avg-qual = 20, strand-filter = 0. Only variants with prevalence higher than 60% were voted as mutations. Following variant calling, mutations were also manually inspected within the aligned reads, and adapted lines that become hypermutators (i.e., that are accumulated more than 55 mutations in a single lineage) were excluded from further analysis. Finally, the annotation of each mutation with genomic features was performed with the intersect subcommand of bedtools v2.25.0.

***In vitro* growth rate measurements.** We measured the growth phenotype of bacterial variants by assessing their growth at 37°C in MHBII medium. To measure growth, we inoculated 5 × 10^4 cells from early stationary-phase cultures (prepared in MHBII medium) into 100 μl of MHBII medium in a 96-well microtiter plate and monitored growth for 24 h. Bacterial growth was measured as the optical density at 600 nm (OD_{600}) of cultures at a given time point. OD_{600} measurements were carried out every 5 min using a BioTek Synergy 2 microplate reader, while bacterial cultures were grown at 37°C under continuous variable-intensity shaking. Each bacterial variant and their corresponding wild types were measured in two consecutive experiments, with 12 replicates in each subsequent test (24 biological replicates in

total). Finally, growth rates were calculated from the obtained growth curves according to a previously described procedure (68, 69).

Competition-based fitness measurements. Competition assay-based fitness measurements were carried out by competing mutant strains against their corresponding wild-type strain carrying a *lacZ* knockout mutation. The *lacZ* knockout strain was constructed by integrating a premature stop codon in place the 23rd amino acid of LacZ with a previously reported pORTMAGE protocol (61). Briefly, heat-induced pORTMAGE3 (Addgene no. 72678) containing *Klebsiella pneumoniae* ATCC 10031 cells was electroporated with KpLacZW23* oligonucleotide (2.5 μM final concentration). Following oligonucleotide integration into the bacterial chromosome, *lacZ*-deficient variants were identified by plating cells out to X-Gal plus IPTG-containing MHBII agar plates at appropriate dilution to form single colonies, where knockout mutants formed white colonies and could be easily distinguished from the dark-blue colonies of the wild type containing a functional β-galactosidase gene. Each competition experiment started by inoculating early stationary-phase cultures in a 99:1 mutant-to-wild-type ratio into 10 ml MHBII medium at a 1:1,000 dilution and incubating each culture at 37°C for 24 h under a constant agitation of 250 rpm. These cultures were then serially transferred into 10 ml fresh MHBII medium in a 1:1,000 dilution every 24 h for 3 subsequent transfers. To analyze the composition of each population, cultures were plated onto MHBII agar plates supplemented with X-Gal and IPTG (in 145 by 20-mm petri dishes; Greiner Bio-One Ltd.) at appropriate dilutions to obtain approximately 1,000 colonies per each plate. The plates were then incubated at 37°C overnight. The ratio of the mutant (*lacZ* proficient, blue colonies) and the wild type (*lacZ* deficient, white colonies) at each given time point was determined from the number of blue and white colonies on X-Gal plus IPTG agar plates. Importantly, prior experiments showed that *lacZ*-deficient *K. pneumoniae* cells suffer no competitive disadvantage compared to their corresponding wild-type strain. Competition experiments were performed in five replicates. Finally, selection coefficients were estimated as the slope of the change in ratio, as defined in the following equation:

$$\ln[\mathrm{x}1(t)/\mathrm{x}2(t)] = \ln[\mathrm{x}1(0)/\mathrm{x}2(0)] + st$$

where *s* is the selection coefficient, *t* is time or number of generations, and x1 and x2 are the ratios of the two strains at a given time point (70).

Prevalence of mutations associated with reduced susceptibility to gepotidacin in sequence databases. In order to investigate if genotypes GyrA D82 and ParC D79N exist in bacteria, we downloaded all DNA sequences from the NCBI nucleotide database by using the following query: ftp://ftp.ncbi.nlm.nih.gov/blast/db/nt.??.tar.gz in wget 1.17.1 on 9 October 2018. We performed the BLAST search with tBLASTn 2.231 (71) (build 7 January 2016) on the downloaded full-nucleotide database as the subject and GyrA and ParC as the query. The protein sequences of GyrA (GenPept accession no. P0AES4) and ParC (GenPept accession no. P0AFI2) were downloaded from UniProt. To perform BLAST, the database was fragmented, and the BLAST search was carried out on these smaller data sets (with argument max_target_seqs = 20,000). Separately obtained results were merged. Finally, for each sequence, the taxonomy of the source bacteria was assigned with blastdbcmd (version 2.2.31).

Mouse thigh infection models. Drug-resistant *K. pneumoniae* is frequently responsible for wound and systemic infections; therefore, we benchmarked the *in vivo* effects of reduced susceptibility to gepotidacin in a murine thigh wound infection model (28, 29). Specifically, we examined wound colonization for representative gepotidacin- and ciprofloxacin-resistant mutants of *K. pneumoniae* ATCC 10031 and compared it to that of the wild type. Murine thigh infections were performed according to a previously established protocol (29, 72). Bacterial inocula were prepared by inoculating single bacterial colonies into 5 ml of MHBII broth and were incubated at 37°C for 16 h under constant agitation (250 rpm). Next, 1/2 volume of a 50% (vol/vol) glycerol-water mixture was added to each culture, and 550 μl of these cell suspensions was frozen at −80°C. Before inoculation, cell suspensions were allowed to thaw at room temperature for 15 min. As test animals, groups of 5 female specific-pathogen-free ICR (CD-1) mice weighing 22 ± 2 g were used. Animals were immunosuppressed by two intraperitoneal injections of cyclophosphamide, the first at 150 mg/kg of body weight 4 days before infection (day −4) and the second at 100 mg/kg 1 day before infection (day −1). On day 0, animals were inoculated intramuscularly into the right thigh with 10^6 CFU/mouse of the corresponding pathogenic mutant (0.1 ml culture/thigh). After 26 h of inoculation, animals were humanely euthanized with CO_2 asphyxiation, and then the muscle of the right thigh was harvested from each test animal. The removed muscle was homogenized in 3 ml of phosphate-buffered saline (pH 7.4) with a polytron homogenizer. Finally, 0.1 ml of these homogenates was used for serial 10-fold dilutions and plated onto LB agar for colony count (CFU per gram) determination.

All aspects of this work, including housing, experimentation, and animal disposal, were performed in general accordance with the Guide for the care and use of laboratory animals (79). All experiments were performed under animal biosafety level 2 (ABSL2) conditions in the American Association for Accreditation of Laboratory Animal Care (AAALAC)-accredited vivarium of Eurofins Pharmacology Discovery Services Taiwan, Ltd. with the oversight of veterinarians to ensure compliance with IACUC regulations and the humane treatment of laboratory animals.

MIC measurements. MICs were determined using a standard serial broth microdilution technique according to the EUCAST guidelines (ISO 20776-1:2006, part 1 [73, 74]). Briefly, bacterial strains were inoculated from frozen cultures onto MHBII agar plates and were grown overnight at 37°C. Next, independent colonies from each strain were inoculated into 1 ml of MHBII medium and were propagated at 37°C and 250 rpm overnight. To perform MIC assays, 12-step serial dilutions using 2-fold dilution steps of the given antibiotic were generated in 96-well microtiter plates (Sarstedt 96-well microtest plate with lid, flat base). Antibiotics were diluted in 100 μl of MHBII medium. Following dilutions, each well was seeded with an inoculum of 5×10^4 bacterial cells. Each measurement was performed in at least 3

parallel replicates. Also, to avoid possible edge effects at the edge of the microwell plate, side rows (A and H) contained only medium without bacterial cells. Following inoculations, the plates were covered with lids and wrapped in polyethylene plastic bags to minimize evaporation but allow for aerobic O_2 transfer. Plates were incubated at 37°C under continuous shaking at 150 rpm for 18 h in an Infors HT shaker. After incubation, the OD_{600} of each well on the microwell plate was measured using a Biotek Synergy 2 microplate reader. The MIC was defined as the antibiotic concentration which inhibited the growth of the bacterial culture, i.e., the drug concentration where the average OD_{600} increment of the three replicates was below 0.05.

SUPPLEMENTAL MATERIAL

ACKNOWLEDGMENTS

REFERENCES

1. Spellberg B, Powers JH, Brass EP, Miller LG, Edwards JE, Jr. 2004. Trends in antimicrobial drug development: implications for the future. Clin Infect Dis 38:1279–1286. https://doi.org/10.1086/420937.
2. Jackson N, Czaplewski L, Piddock LJ. 2018. Discovery and development of new antibacterial drugs: learning from experience? J Antimicrob Chemother 73:1452–1459. https://doi.org/10.1093/jac/dky019.
3. Suzuki S, Horinouchi T, Furusawa C. 2015. Suppression of antibiotic resistance acquisition by combined use of antibiotics. J Biosci Bioeng 120:467–469. https://doi.org/10.1016/j.jbiosc.2015.02.003.
4. Munck C, Gumpert HK, Wallin AIN, Wang HH, Sommer M. 2014. Prediction of resistance development against drug combinations by collateral responses to component drugs. Sci Transl Med 6:262ra156. https://doi .org/10.1126/scitranslmed.3009940.
5. Silver LL. 2007. Multi-targeting by monotherapeutic antibacterials. Nat Rev Drug Discov 6:41–55. https://doi.org/10.1038/nrd2202.
6. Klahn P, Brönstrup M. 2017. Bifunctional antimicrobial conjugates and hybrid antimicrobials. Nat Prod Rep 34:832–885. https://doi.org/10.1039/C7NP00006E.
7. Eliopoulos GM, Meka VG, Gold HS. 2004. Antimicrobial resistance to linezolid. Clin Infect Dis 39:1010–1015. https://doi.org/10.1086/423841.
8. Farrell DJ, Sader HS, Rhomberg PR, Scangarella-Oman NE, Flamm RK. 2017. In vitro activity of gepotidacin (GSK2140944) against Neisseria gonorrhoeae. Antimicrob Agents Chemother 61:e02047-16. https://doi .org/10.1128/AAC.02047-16.
9. Dougherty TJ, Nayar A, Newman JV, Hopkins S, Stone GG, Johnstone M, Shapiro AB, Cronin M, Reck F, Ehmann DE. 2014. NBTI 5463 is a novel bacterial type II topoisomerase inhibitor with activity against Gram-negative bacteria and in vivo efficacy. Antimicrob Agents Chemother 58:2657–2664. https://doi.org/10.1128/AAC.02778-13.
10. Tari LW, Li X, Trzoss M, Bensen DC, Chen Z, Lam T, Zhang J, Lee SJ, Hough G, Phillipson D, Akers-Rodriguez S, Cunningham ML, Kwan BP, Nelson KJ, Castellano A, Locke JB, Brown-Driver V, Murphy TM, Ong VS, Pillar CM, Shinabarger DL, Nix J, Lightstone FC, Wong SE, Nguyen TB, Shaw KJ, Finn J. 2013. Tricyclic GyrB/ParE (TriBE) inhibitors: a new class of broad-spectrum dual-targeting antibacterial agents. PLoS One 8:e84409. https://doi.org/10.1371/journal.pone.0084409.
11. Wang KK, Stone LK, Lieberman TD, Shavit M, Baasov T, Kishony R. 2016. A hybrid drug limits resistance by evading the action of the multiple antibiotic resistance pathway. Mol Biol Evol 33:492–500. https://doi.org/10.1093/molbev/msv243.
12. Pokrovskaya V, Belakhov V, Hainrichson M, Yaron S, Baasov T. 2009. Design, synthesis, and evaluation of novel fluoroquinolone−aminoglycoside hybrid antibiotics. J Med Chem 52:2243–2254. https://doi.org/10 .1021/jm900028n.
13. Nayar AS, Dougherty TJ, Reck F, Thresher J, Gao N, Shapiro AB, Ehmann DE. 2015. Target-based resistance in Pseudomonas aeruginosa and Escherichia coli to NBTI 5463, a novel bacterial type II topoisomerase inhib-

itor. Antimicrob Agents Chemother 59:331–337. https://doi.org/10.1128/AAC.04077-14.

14. Taylor SN, Morris DH, Avery AK, Workowski KA, Batteiger BE, Tiffany CA, Perry CR, Raychaudhuri A, Scangarella-Oman NE, Hossain M, Dumont EF. 2018. Gepotidacin for the treatment of uncomplicated urogenital gonorrhea: a phase 2, randomized, dose-ranging, single-oral dose evaluation. Clin Infect Dis 67:504–512. https://doi.org/10.1093/cid/ciy145.

15. O'Riordan W, Tiffany C, Scangarella-Oman N, Perry C, Hossain M, Ashton T, Dumont E. 2017. The efficacy, safety, and tolerability of gepotidacin (GSK2140944) in the treatment of patients with suspected or confirmed Gram-positive acute bacterial skin and skin structure infections. Antimicrob Agents Chemother 61:e02095-16. https://doi.org/10.1128/AAC.02095-16.

16. Biedenbach DJ, Bouchillon SK, Hackel M, Miller LA, Scangarella-Oman NE, Jakielaszek C, Sahm DF. 2016. In vitro activity of gepotidacin, a novel triazaacenaphthylene bacterial topoisomerase inhibitor, against a broad spectrum of bacterial pathogens. Antimicrob Agents Chemother 60:1918–1923. https://doi.org/10.1128/AAC.02820-15.

17. Flamm RK, Farrell DJ, Rhomberg PR, Scangarella-Oman NE, Sader HS. 2017. Gepotidacin (GSK2140944) in vitro activity against Gram-positive and Gram-negative bacteria. Antimicrob Agents Chemother 61:e00468-17. https://doi.org/10.1128/AAC.00468-17.

18. Nyerges Á, Csörgő B, Draskovits G, Kintses B, Szili P, Ferenc G, Révész T, Ari E, Nagy I, Bálint B, Vásárhelyi BM, Bihari P, Számel M, Balogh D, Papp H, Kalapis D, Papp B, Pál C. 2018. Directed evolution of multiple genomic loci allows the prediction of antibiotic resistance. Proc Natl Acad Sci U S A 115:E5726–E5735. https://doi.org/10.1073/pnas.1801646115.

19. Tillotson G. 2018. A crucial list of pathogens. Lancet Infect Dis 18:234–236. https://doi.org/10.1016/S1473-3099(17)30754-5.

20. Kollman PA, Massova I, Reyes C, Kuhn B, Huo S, Chong L, Lee M, Lee T, Duan Y, Wang W, Donini O, Cieplak P, Srinivasan J, Case DA, Cheatham TE, III. 2000. Calculating structures and free energies of complex molecules: combining molecular mechanics and continuum models. Acc Chem Res 33:889–897. https://doi.org/10.1021/ar000033j.

21. Hughes D, Andersson DI. 2015. Evolutionary consequences of drug resistance: shared principles across diverse targets and organisms. Nat Rev Genet 16:459–471. https://doi.org/10.1038/nrg3922.

22. Martínez JL, Baquero F, Andersson DI. 2011. Beyond serial passages: new methods for predicting the emergence of resistance to novel antibiotics. Curr Opin Pharmacol 11:439–445. https://doi.org/10.1016/j.coph.2011.07.005.

23. Sommer MO, Munck C, Toft-Kehler RV, Andersson DI. 2017. Prediction of antibiotic resistance: time for a new preclinical paradigm? Nat Rev Microbiol 15:689. https://doi.org/10.1038/nrmicro.2017.75.

24. Andersson DI. 2015. Improving predictions of the risk of resistance development against new and old antibiotics. Clin Microbiol Infect 21:894–898. https://doi.org/10.1016/j.cmi.2015.05.012.

25. Krapp F, Ozer EA, Qi C, Hauser AR. 2018. Case report of an extensively drug-resistant Klebsiella pneumoniae infection with genomic characterization of the strain and review of similar cases in the United States. Open Forum Infect Dis 5: ofy074. https://doi.org/10.1093/ofid/ofy074.

26. Weigel LM, Steward CD, Tenover FC. 1998. gyrA mutations associated with fluoroquinolone resistance in eight species of Enterobacteriaceae. Antimicrob Agents Chemother 42:2661–2667. https://doi.org/10.1128/AAC.42.10.2661.

27. Chen F-J, Lauderdale T-L, Ho M, Lo H-J. 2003. The roles of mutations in gyrA, parC, and ompK35 in fluoroquinolone resistance in Klebsiella pneumoniae. Microb Drug Resist 9:265–271. https://doi.org/10.1089/107662903322286472.

28. Velkov T, Bergen PJ, Lora-Tamayo J, Landersdorfer CB, Li J. 2013. PK/PD models in antibacterial development. Curr Opin Microbiol 16:573–579. https://doi.org/10.1016/j.mib.2013.06.010.

29. Tan CM, Therien AG, Lu J, Lee SH, Caron A, Gill CJ, Lebeau-Jacob C, Benton-Perdomo L, Monteiro JM, Pereira PM, Elsen NL, Wu J, Deschamps K, Petcu M, Wong S, Daigneault E, Kramer S, Liang L, Maxwell E, Claveau D, Vaillancourt J, Skorey K, Tam J, Wang H, Meredith TC, Sillaots S, Wang-Jarantow L, Ramtohul Y, Langlois E, Landry F, Reid JC, Parthasarathy G, Sharma S, Baryshnikova A, Lumb KJ, Pinho MG, Soisson SM, Roemer T. 2012. Restoring methicillin-resistant Staphylococcus aureus susceptibility to β-lactam antibiotics. Sci Transl Med 4:126ra35. https://doi.org/10.1126/scitranslmed.3003592.

30. Hooper DC, Jacoby GA. 2016. Topoisomerase inhibitors: fluoroquinolone mechanisms of action and resistance. Cold Spring Harb Perspect Med 6:a025320. https://doi.org/10.1101/cshperspect.a025320.

31. Gibson EG, Ashley RE, Kerns RJ, Osheroff N. 2018. Bacterial type II topoisomerases and target-mediated drug resistance, p 507–529. In Fong IW, Shlaes D, Drlica K (ed), Antimicrobial resistance in the 21st century. Springer International Publishing, Cham, Switzerland.

32. Wohlkonig A, Chan PF, Fosberry AP, Homes P, Huang J, Kranz M, Leydon VR, Miles TJ, Pearson ND, Perera RL, Shillings AJ, Gwynn MN, Bax BD. 2010. Structural basis of quinolone inhibition of type IIA topoisomerases and target-mediated resistance. Nat Struct Mol Biol 17:1152–1153. https://doi.org/10.1038/nsmb.1892.

33. Collin F, Karkare S, Maxwell A. 2011. Exploiting bacterial DNA gyrase as a drug target: current state and perspectives. Appl Microbiol Biotechnol 92:479–497. https://doi.org/10.1007/s00253-011-3557-z.

34. Correia S, Poeta P, Hébraud M, Capelo JL, Igrejas G. 2017. Mechanisms of quinolone action and resistance: where do we stand? J Med Microbiol 66:551–559. https://doi.org/10.1099/jmm.0.000475.

35. Scangarella-Oman NE, Hossain M, Dixon PB, Ingraham K, Min S, Tiffany CA, Perry CR, Raychaudhuri A, Dumont EF, Huang J, Hook EW, III, Miller LA. 2018. Microbiological analysis from a phase 2 randomized study in adults evaluating single oral doses of gepotidacin in the treatment of uncomplicated urogenital gonorrhea caused by Neisseria gonorrhoeae. Antimicrob Agents Chemother 62:e01221-18. https://doi.org/10.1128/AAC.01221-18.

36. Bell G, MacLean C. 2018. The search for 'evolution-proof' antibiotics. Trends Microbiol 26:471–483. https://doi.org/10.1016/j.tim.2017.11.005.

37. Martínez JL, Baquero F, Andersson DI. 2007. Predicting antibiotic resistance. Nat Rev Microbiol 5:958–965. https://doi.org/10.1038/nrmicro1796.

38. Lázár V, Martins A, Spohn R, Daruka L, Grézal G, Fekete G, Számel M, Jangir PK, Kintses B, Csörgő B, Nyerges Á, Györkei Á, Kincses A, Dér A, Walter FR, Deli MA, Urbán E, Hegedűs Z, Olajos G, Méhi O, Bálint B, Nagy I, Martinek TA, Papp B, Pál C. 2018. Antibiotic-resistant bacteria show widespread collateral sensitivity to antimicrobial peptides. Nat Microbiol 3:718–731. https://doi.org/10.1038/s41564-018-0164-0.

39. Baym M, Lieberman TD, Kelsic ED, Chait R, Gross R, Yelin I, Kishony R. 2016. Spatiotemporal microbial evolution on antibiotic landscapes. Science 353:1147–1151. https://doi.org/10.1126/science.aag0822.

40. European Committee on Antimicrobial Susceptibility Testing. 2018. EUCAST: Clinical breakpoints. European Committee on Antimicrobial Susceptibility Testing, Växjö, Sweden. http://www.eucast.org/fileadmin/src/media/PDFs/EUCAST_files/Breakpoint_tables/v_9.0_Breakpoint_Tables.pdf.

41. Miles TJ, Hennessy AJ, Bax B, Brooks G, Brown BS, Brown P, Cailleau N, Chen D, Dabbs S, Davies DT, Esken JM, Giordano I, Hoover JL, Jones GE, Kusalakumari Sukmar SK, Markwell RE, Minthorn EA, Rittenhouse S, Gwynn MN, Pearson ND. 2016. Novel tricyclics (e.g., GSK945237) as potent inhibitors of bacterial type IIA topoisomerases. Bioorg Med Chem Lett 26:2464–2469. https://doi.org/10.1016/j.bmcl.2016.03.106.

42. Harkins CP, Pichon B, Doumith M, Parkhill J, Westh H, Tomasz A, de Lencastre H, Bentley SD, Kearns AM, Holden MT. 2017. Methicillin-resistant Staphylococcus aureus emerged long before the introduction of methicillin into clinical practice. Genome Biol 18:130. https://doi.org/10.1186/s13059-017-1252-9.

43. Marcusson LL, Frimodt-Møller N, Hughes D. 2009. Interplay in the selection of fluoroquinolone resistance and bacterial fitness. PLoS Pathog 5:e1000541. https://doi.org/10.1371/journal.ppat.1000541.

44. Hooper DC, Jacoby GA. 2015. Mechanisms of drug resistance: quinolone resistance. Ann N Y Acad Sci 1354:12–31. https://doi.org/10.1111/nyas.12830.

45. Weinstein ZB, Zaman MH. 2018. Evolution of rifampicin resistance due to substandard drugs in E. coli and M. smegmatis. Antimicrob Agents Chemother 63:01243-18. https://doi.org/10.1128/AAC.01243-18.

46. Van Boeckel TP, Gandra S, Ashok A, Caudron Q, Grenfell BT, Levin SA, Laxminarayan R. 2014. Global antibiotic consumption 2000 to 2010: an analysis of national pharmaceutical sales data. Lancet Infect Dis 14:742–750. https://doi.org/10.1016/S1473-3099(14)70780-7.

47. Taylor SN, Marrazzo J, Batteiger BE, Hook EW, Seña AC, Long J, Wierzbicki MR, Kwak H, Johnson SM, Lawrence K, Mueller J. 2018. Single-dose zoliflodacin (ETX0914) for treatment of urogenital gonorrhea. N Engl J Med 379:1835–1845. https://doi.org/10.1056/NEJMoa1706988.

48. Basarab GS, Kern GH, McNulty J, Mueller JP, Lawrence K, Vishwanathan K, Alm RA, Barvian K, Doig P, Galullo V, Gardner H, Gowravaram M, Huband M, Kimzey A, Morningstar M, Kutschke A, Lahiri SD, Perros M, Singh R, Schuck VJA, Tommasi R, Walkup G, Newman JV. 2015. Responding to the challenge of untreatable gonorrhea: ETX0914, a first-in-class agent with a distinct mechanism-of-action against bacterial type II topoisomerases. Sci Rep 5:11827. https://doi.org/10.1038/srep11827.

49. Foerster S, Golparian D, Jacobsson S, Hathaway LJ, Low N, Shafer WM, Althaus CL, Unemo M. 2015. Genetic resistance determinants, in vitro time-kill curve analysis and pharmacodynamic functions for the novel topoisomerase II inhibitor ETX0914 (AZD0914) in Neisseria gonorrhoeae. Front Microbiol 6:1377. https://doi.org/10.3389/fmicb.2015.01377.

50. Damião Gouveia AC, Unemo M, Jensen JS. 2018. In vitro activity of zoliflodacin (ETX0914) against macrolide-resistant, fluoroquinolone-resistant and antimicrobial-susceptible Mycoplasma genitalium strains. J Antimicrob Chemother 73:1291–1294. https://doi.org/10.1093/jac/dky022.

51. Schrödinger, LLC. 2017. Small-Molecule Drug Discovery Suite 2017-4. Schrödinger, LLC, New York, NY.

52. Harder E, Damm W, Maple J, Wu C, Reboul M, Xiang JY, Wang L, Lupyan D, Dahlgren MK, Knight JL, Kaus JW, Cerutti DS, Krilov G, Jorgensen WL, Abel R, Friesner RA. 2016. OPLS3: a force field providing broad coverage of drug-like small molecules and proteins. J Chem Theory Comput 12:281–296. https://doi.org/10.1021/acs.jctc.5b00864.

53. Berendsen HJC, Postma JPM, van Gunsteren WF, Hermans J. 1981. Interaction models for water in relation to protein hydration, p 331–342. In Pullman B (ed), Intermolecular forces. Springer Netherlands, Dordrecht, the Netherlands.

54. Bowers KJ, Chow DE, Xu H, Dror RO, Eastwood MP, Gregersen BA, Klepeis JL, Kolossvary I, Moraes MA, Sacerdoti FD, Salmon JK, Shan Y, Shaw DE. 2006. Scalable algorithms for molecular dynamics simulations on commodity clusters. SC '06: proceedings of the 2006 ACM/IEEE Conference on Supercomputing, Tampa, FL.

55. Schrödinger, LLC. 2017. Schrödinger release 2017-4: Bioluminate. Schrödinger, LLC, New York, NY.

56. Sirin S, Pearlman DA, Sherman W. 2014. Physics-based enzyme design: predicting binding affinity and catalytic activity. Proteins 82:3397–3409. https://doi.org/10.1002/prot.24694.

57. Chrencik JE, Roth CB, Terakado M, Kurata H, Omi R, Kihara Y, Warshaviak D, Nakade S, Asmar-Rovira G, Mileni M, Mizuno H, Griffith MT, Rodgers C, Han GW, Velasquez J, Chun J, Stevens RC, Hanson MA. 2015. Crystal structure of antagonist bound human lysophosphatidic acid receptor 1. Cell 161:1633–1643. https://doi.org/10.1016/j.cell.2015.06.002.

58. Krishnamurthy VR, Sardar MYR, Ying Y, Song X, Haller C, Dai E, Wang X, Hanjaya-Putra D, Sun L, Morikis V, Simon SI, Woods RJ, Cummings RD, Chaikof EL. 2015. Glycopeptide analogues of PSGL-1 inhibit P-selectin in vitro and in vivo. Nat Commun 6:6387. https://doi.org/10.1038/ncomms7387.

59. Lyne PD, Lamb ML, Saeh JC. 2006. Accurate prediction of the relative potencies of members of a series of kinase inhibitors using molecular docking and MM-GBSA scoring. J Med Chem 49:4805–4808. https://doi.org/10.1021/jm060522a.

60. Greenidge PA, Kramer C, Mozziconacci J-C, Wolf RM. 2013. MM/GBSA binding energy prediction on the PDBbind data set: successes, failures, and directions for further improvement. J Chem Inf Model 53:201–209. https://doi.org/10.1021/ci300425v.

61. Nyerges Á, Csörgő B, Nagy I, Bálint B, Bihari P, Lázár V, Apjok G, Umenhoffer K, Bogos B, Pósfai G, Pál C. 2016. A highly precise and portable genome engineering method allows comparison of mutational effects across bacterial species. Proc Natl Acad Sci U S A 113:2502–2507. https://doi.org/10.1073/pnas.1520040113.

62. Ricaurte DE, Martínez-García E, Nyerges Á, Pál C, de Lorenzo V, Aparicio T. 2018. A standardized workflow for surveying recombinases expands bacterial genome-editing capabilities. Microb Biotechnol 11:176–188. https://doi.org/10.1111/1751-7915.12846.

63. Jiang W, Bikard D, Cox D, Zhang F, Marraffini LA. 2013. RNA-guided editing of bacterial genomes using CRISPR-Cas systems. Nat Biotechnol 31:233–239. https://doi.org/10.1038/nbt.2508.

64. Umenhoffer K, Draskovits G, Nyerges Á, Karcagi I, Bogos B, Tímár E, Csörgő B, Herczeg R, Nagy I, Fehér T, Pál C, Pósfai G. 2017. Genome-wide abolishment of mobile genetic elements using genome shuffling and CRISPR/Cas-assisted MAGE allows the efficient stabilization of a bacterial chassis. ACS Synth Biol 6:1471–1483. https://doi.org/10.1021/acssynbio.6b00378.

65. Bódi Z, Farkas Z, Nevozhay D, Kalapis D, Lázár V, Csörgő B, Nyerges Á, Szamecz B, Fekete G, Papp B, Araújo H, Oliveira JL, Moura G, Santos MAS, Székely T, Jr, Balázsi G, Pál C. 2017. Phenotypic heterogeneity promotes adaptive evolution. PLoS Biol 15:e2000644. https://doi.org/10.1371/journal.pbio.2000644.

66. Li H, Durbin R. 2009. Fast and accurate short read alignment with Burrows-Wheeler transform. Bioinformatics 25:1754–1760. https://doi.org/10.1093/bioinformatics/btp324.

67. Koboldt DC, Zhang Q, Larson DE, Shen D, McLellan MD, Lin L, Miller CA, Mardis ER, Ding L, Wilson RK. 2012. VarScan 2: somatic mutation and copy number alteration discovery in cancer by exome sequencing. Genome Res 22:568–576. https://doi.org/10.1101/gr.129684.111.

68. Warringer J, Ericson E, Fernandez L, Nerman O, Blomberg A. 2003. High-resolution yeast phenomics resolves different physiological features in the saline response. Proc Natl Acad Sci U S A 100:15724–15729. https://doi.org/10.1073/pnas.2435976100.

69. Karcagi I, Draskovits G, Umenhoffer K, Fekete G, Kovács K, Méhi O, Balikó G, Szappanos B, Györfy Z, Fehér T, Bogos B, Blattner FR, Pál C, Pósfai G, Papp B. 2016. Indispensability of horizontally transferred genes and its impact on bacterial genome streamlining. Mol Biol Evol 33:1257–1269. https://doi.org/10.1093/molbev/msw009.

70. Dykhuizen DE. 1990. Experimental studies of natural selection in bacteria. Annu Rev Ecol Syst 21:373–398. https://doi.org/10.1146/annurev.es.21.110190.002105.

71. Altschul SF, Gish W, Miller W, Myers EW, Lipman DJ. 1990. Basic local alignment search tool. J Mol Biol 215:403–410. https://doi.org/10.1016/S0022-2836(05)80360-2.

72. DeRyke CA, Banevicius MA, Fan HW, Nicolau DP. 2007. Bactericidal activities of meropenem and ertapenem against extended-spectrum-β-lactamase-producing Escherichia coli and Klebsiella pneumoniae in a neutropenic mouse thigh model. Antimicrob Agents Chemother 51:1481–1486. https://doi.org/10.1128/AAC.00752-06.

73. International Organization for Standardization (ISO). 2006. ISO 20776-1: 2006 Clinical laboratory testing and in vitro diagnostic test systems–susceptibility testing of infectious agents and evaluation of performance of antimicrobial susceptibility test devices–part 1: reference method for testing the in vitro activity of antimicrobial agents against rapidly growing aerobic bacteria involved in infectious diseases. International Organization for Standardization, Geneva, Switzerland.

74. European Committee on Antimicrobial Susceptibility Testing. 2018. EUCAST recommendations: MIC determination of non-fastidious and fastidious organisms. European Committee on Antimicrobial Susceptibility Testing, Växjö, Sweden. http://www.eucast.org/ast_of_bacteria/mic_determination.

75. Chan PF, Germe T, Bax BD, Huang J, Thalji RK, Bacque E, Checchia A, Chen D, Cui H, Ding X, Ingraham K, McCloskey L, Raha K, Srikannathasan V, Maxwell A, Stavenger RA. 2017. Thiophene antibacterials that allosterically stabilize DNA-cleavage complexes with DNA gyrase. Proc Natl Acad Sci U S A 114:E4492–E4500. https://doi.org/10.1073/pnas.1700721114.

76. Jacobson MP, Friesner RA, Xiang Z, Honig B. 2002. On the role of the crystal environment in determining protein side-chain conformations. J Mol Biol 320:597–608. https://doi.org/10.1016/s0022-2836(02)00470-9.

77. Jacobson MP, Pincus DL, Rapp CS, Day TJF, Honig B, Shaw DE, Friesner RA. 2004. A hierarchical approach to all-atom protein loop prediction. Proteins 55:351–367. https://doi.org/10.1002/prot.10613.

78. Veselkov DA, Laponogov I, Pan X-S, Selvarajah J, Skamrova GB, Branstrom A, Narasimhan J, Prasad JVNV, Fisher LM, Sanderson MR. 2016. Structure of a quinolone-stabilized cleavage complex of topoisomerase IV from Klebsiella pneumoniae and comparison with a related Streptococcus pneumoniae complex. Acta Crystallogr D Struct Biol 72:488–496. https://doi.org/10.1107/S2059798316001212.

79. Committee for the Update of the Guide for the Care and Use of Laboratory Animals. 2011. Guide for the care and use of laboratory animals, 8th ed. National Academy Press, Washington, DC.